NEW SEISMIC CONSTRUCTION CATEGORIES FOR REINFORCED CONCRETE BLOCK STRUCTURAL WALLS: EXPERIMENTS

Shedid, Marwan[1]; El-Dakhakhni, Wael[2] and Drysdale, Robert[3]

[1] PhD, Assistant Professor, Ain-Shams University, Cairo, Egypt. shedidmm@mcmaster.ca
[2] PhD, Martini, Mascarin & George Chair in Masonry Design, McMaster Univ., Canada. eldak@mcmaster.ca
[3] PhD, Professor Emeritus, McMaster University, Hamilton, Canada. drysdale@mcmaster.ca

In this paper, a series of reinforced concrete-block shear walls with aspect ratios of 1.5 and 2.2 were tested under displacement-controlled cyclic loading. The response of rectangular, flanged, and end-confined walls, designed to have the same lateral resistance when subjected to the same axial load, is discussed. In general, high levels of ductility accompanied by relatively small strength degradation were observed in all walls with a significant increase in ductility and displacement capabilities for the flanged and end-confined walls compared to the rectangular ones. For both aspect ratios evaluated, the drift levels at 20% strength degradation were 1.0, 1.5, and 2.2% corresponding to the rectangular, the flanged, and the end-confined walls, respectively. The ductility values of the proposed flanged and end-confined walls were, respectively, 1.5 and 2 times those of their rectangular wall counterparts (with the same overall length and aspect ratio). In addition to the enhanced ductility, a saving of more than 40% in the amount of vertical reinforcement was achieved using the proposed alternative strategies while maintaining the same lateral wall resistance. Existing design clauses were used to predict the wall capacities using the American and the Canadian masonry codes and showed excellent agreement. This will facilitate adoption of the new construction categories with minimal modifications to existing code clauses. The test results indicate that higher ductility than the currently endorsed values by North American codes should be used for rectangular walls. Moreover, higher values should be expected when the proposed strategies are adopted which would significantly reduce the seismic demand on reinforced concrete-block shear wall construction.

Keywords: *Boundary elements, Concrete masonry, Ductility, Flanges; Seismic tests; Shear walls.*

INTRODUCTION

The common perception that reinforced masonry (RM) cannot provide high ductility compared to reinforced concrete (RC) may be in part attributed to the poor performance of unreinforced masonry during a series of earthquakes during the 19th and the 20th century such as Imperial Valley (1892), San Fernando (1906), Long Beach (1933), San Fernando (1971) and Northridge (1994) earthquakes that illustrated the seismic vulnerability of unreinforced masonry structures. The need for a more ductile and earthquake-resistant form of masonry construction resulted in the development of RM. Nevertheless, seismic design of RM structures still involves a high level of conservatism in North American codes. Recent experimental investigation (Shing et al. 1990, Seible et al. 1993, Eikanas 2003, and Shedid et al. 2008) concluded that high levels of ductility and small strength degradation, at large drift levels, are to be expected from RM shear walls failing in flexure. However, there is still a

need for applicable research with detailed documentation to support the proposal that RM walls are ductile. Moreover, fundamental research focusing on enhancing the ductility and energy dissipation qualities of masonry structures is required. To enhance the behavior of masonry under in-plane loading, one should first identify the differences between typical RM construction practice and the detailing of ductile RC shear walls. A significant difference between RM and RC walls is the presence of closed ties and two layers of vertical reinforcement in RC walls which provides a reinforcing cage to confine the compression zone, whereas, due to practical limitation associated with concrete block wall cross sections, single horizontal ties and single layer of vertical reinforcement are typically used in RM and, therefore, no confinement is provided at the wall ends. The reinforcement arrangement in RM may lead to instability of the compression zone under high inelastic strains in the vertical bars during cyclic loading. The instability can consist of out-of-plane displacement of the wall and bar buckling in the compression zone (Paulay and Priestley 1992).

The above drawbacks can be resolved and the performance of RM walls may be enhanced by connecting them with boundary elements or flanges. The presence of boundary elements at the end zone of the walls allows the use of more than one layer of vertical bars that can be confined within closed ties. Moreover, structurally connecting a rectangular wall to a small flange (or an intersecting wall) or to a boundary element could limit the damage at the wall ends and provide out-of-plane stability. Also, the increased thickness at the wall ends can significantly decrease the required length of the compression zone leading to increased curvature at maximum load. Therefore, the increased curvature ductility should lead to corresponding increase in the displacement ductility of the wall. In this regards, the response of RC rectangular walls has been shown to be generally enhanced when boundary elements were added at their ends or when walls were structurally connected to intersecting walls (Paulay and Priestley 1992). Surprisingly, very little research has been carried out on the lateral loading performance characteristics of flanged RM walls or RM walls with boundary elements.

There are several discussions in the literature regarding the appropriate definition of displacement ductility for behaviors that are not ideally elastic-plastic (Park and Paulay 1975, Shing et al. 1989, Paulay and Priestley 1992, Priestley et al. 1996, Tomazevic 1998). However, as highlighted by Priestley (2000), and Priestley et al. (2008), there is no general consensus or a unified definition for the yield and the ultimate displacements. Shedid et al. (2010) showed that, for RM shear walls failing in flexure, the wall capacities based on an elastic-plastic idealization of the actual load-displacement response using the equal area approach are, on average, 97% of the measured capacities. This approach will be adopted in this study to quantify and facilitate comparisons between the different wall ductility levels and drift limits associated with the proposed alternative construction strategies. The adoption of such strategies to enhance the seismic performance is expected to significantly reduce the seismic demand on RM building with minimal modification and a significant saving in reinforcement as will be discussed later in the paper.

In the current study, the experimental behavior of seven half-scale fully-grouted RM shear walls, all with the same length but different end configurations and aspect ratios is reported. As the seismic performance is significantly influenced by ductility, the aim of the study was to evaluate and document the enhanced ductile behavior of rectangular RM shear walls when flanges and boundary elements are structurally connected at the wall ends.

WALL DETAILS

For a typical mid-rise masonry building (e.g. 5 storey), wall lengths may vary from 2.0 to 8.0 m resulting in an aspect ratio of at least 1.5, and a wall axial compressive stress ranging from 1.0 to 2.0 MPa (i.e. 0.2 to 0.4 MPa per floor) on average.

Using half-scale blocks, a series of 3-storey and 2-storey high concrete block shear walls with a length 1.8 m (corresponding to 3.6 m length in full-scale) containing 19 cells (9.5 blocks) were constructed. This length allowed for several possible arrangements of vertical reinforcement (e.g. every cell, every other cell, and every third cell). With this length, the aspect ratio of the test walls ranged between 2.2 and 1.5 for the 3-storey and 2-storey high walls, respectively.
The complete test matrix is given in Table 1, where all walls including the rectangular walls (W1 and W4) had the same overall length. The flanged walls (W2 and W5) were constructed using eight and one-half blocks along the web and one and one-half blocks (285 mm) placed orthogonal to the web (i.e. 90 mm at each wall end). The end-confined walls (W3, W6, and W7) were constructed using seven and one-half blocks along the web. The boundary elements for the specimens W3 and W6 were composed of two blocks (185 mm × 90 mm each) placed adjacent to each other, whereas, for the specimen W7, a pilaster unit (185 mm × 185 mm) was used. The cross section for all the test walls is shown in Fig. 1.

Table 1: Wall Test matrix

Specimen	Wall dimensions	Vertical reinforcement		Horizontal reinforcement		Axial stress (MPa)
		Number of bars and bar size	ρ_v (%)	No. D4 @ spacing (mm)	ρ_h (%)	
Phase I						
W1	1,802 mm ×3,990 mm Length × Height	19 M10	1.17	1 @190	0.15	1.09
W2		11 M10	0.55	1 @190	0.15	0.89
W3		11 M10	0.55	1 @190	0.15	0.89
Phase II						
W4	1,802 mm ×2,660 mm Length × Height	19 M10	1.17	2 @95	0.60	1.05
W5		11 M10	0.55	2 @95	0.60	0.88
W6		11 M10	0.55	2 @ 95	0.60	0.88
W7*		11 M10	0.55	2 @ 95	0.60	0.88

*** Spiral reinforcement in the boundary element**

Testing a wall having a compression zone depth greater than one block long was an important criterion in wall dimension and reinforcement selection. This was to ensure that the whole area of the boundary elements or the flanges and that more than one layer of reinforcement are under compression, which would more realistically represent a wall response compared to that of a beam. In addition, to represent shear wall behavior when governed by flexure, a reasonable aspect ratio was also a controlling condition in the selection of the wall dimensions.
The test program consisted of two phases: Phase I included the 3-storey high walls and Phase II included the 2-storey high walls. All walls in each phase had the same overall length and were designed to have the same lateral load capacity (at the ultimate masonry compressive strain) while being under the same magnitude of axial compressive load (i.e. resulting from the same tributary floor area). This was the most important design criterion selected to illustrate the effect of adding boundary elements and flanges on the cyclic behavior, ductility, and post-peak response of rectangular walls when these walls are replaced by flanged or end-confined walls (having the same overall length and capacity under the same axial compression load). Designing the flanged and end-confined walls to have the same lateral capacity of a rectangular wall having same overall length and height resulted in a reduction of about 43% in the amount of vertical reinforcement (the number of bars dropped from 19 to 11).

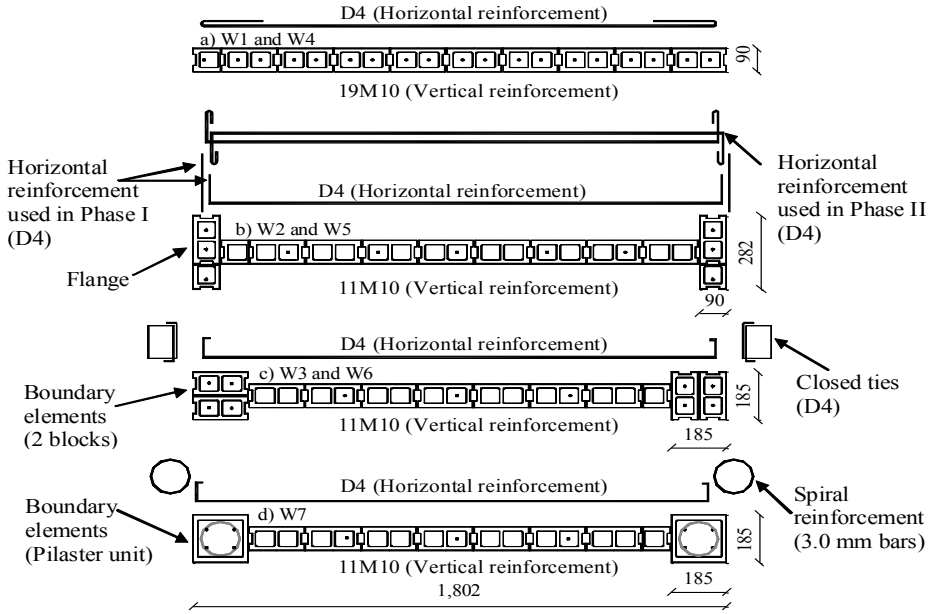

Fig. 1: Cross-section of the test walls (all dimensions are in mm)

WALL CONSTRUCTION AND TEST SETUP

An experienced mason constructed all wall specimens in a running bond pattern with face shell mortar bedding using half-scale (5 mm) mortar joints. The walls in Phase I were 39 courses high (13 courses per storey) and had three 100 mm thick RC slabs, whereas in Phase II, the walls were 26 courses high and had 2 RC slabs.

D4 bars (area = 25.4 mm^2) which are the half-scale equivalent of the full-scale M10 reinforcing bars (area = 100 mm^2), were used as horizontal reinforcement and were fitted along the existing notch in the webs of the half-scale blocks. In the flanged and end-confined walls, the face shells of the blocks located in the boundary elements, the flanges, and the pilaster units were saw-cut to a 20 mm depth to accommodate the horizontal shear reinforcement. This construction detail resulted in forming a large continuous horizontal cell that accommodated the shear reinforcement along the entire wall length and provided full embedment of the reinforcement in the grout.

The horizontal reinforcement in the rectangular walls formed 180° hooks around the outermost vertical reinforcement. The 200 mm return leg of the hook extended to the third last cell as shown in Fig. 1 (a) to provide adequate development length. For the flanged wall in Phase I, the horizontal reinforcement along the web was bent 90° in the flanges (see Fig. 1 (b)). Based on the observed failure mode of the flanged wall during Phase I, the horizontal reinforcement in Phase II, was bent 90° in the flange and then 180° around the outermost reinforcement in the flange (see Fig. 1 (b)). For the end-confined walls, the horizontal reinforcement along the web was developed inside the boundary element zone and was bent 90° around one of the outermost vertical bars (Fig. 1 (c) and 1 (d)). For the boundary elements constructed using the half-scale blocks, closed ties were provided around the 4 end bars as shown in Fig. 1 (c), whereas, spiral reinforcement, with 30 mm pitch, was used within the pilaster unit (Fig. 1 (d)). A summary of the wall reinforcement ratios, number of bars, and level of applied axial stress is given in Table 1.

The vertical and horizontal reinforcement ratios, ρ_v and ρ_h, are described as percentages of the gross areas of the horizontal and vertical wall cross section, respectively. To account for the reduced masonry shear strength in the expected plastic hinge region close to the base, the horizontal reinforcement indicated in Table 1 was doubled over the first storey for walls tested in Phase I (D4 bar in every course versus every other course). On the other hand, the horizontal

reinforcement was maintained the same in both floors for walls tested in Phase II as an area equivalent to 1.1 times the area of a D4 bar in every course was needed in the second floor (outside the expected plastic hinge zone). This resulted in using two D4 bars every course throughout the height of the walls tested in Phase II.

MATERIALS

A half-scale version of the standard 200 mm hollow concrete block (190 mm depth ×190 mm width ×390 mm length) was used for construction of the test walls. Half-scale blocks were tested in accordance with the CSA A165.1 (CSA 2004a) using hard capping and 120 mm thick loading plates. The average compressive strength for concrete masonry blocks, based on net area (8,490 mm^2), was 27.2 MPa (*c.o.v.* = 7.1%). Fine grout with an average cylinder compressive strength of 21.8 MPa (*c.o.v. = 15.7%)* was used for the walls. The concrete used in the wall foundation and storey slabs had an average compressive strength of 27.3 MPa (*c.o.v.* = 2.8%) and 36.0 MPa (*c.o.v. = 7.6%),* respectively.

Three four-block high by one block long (375 mm high ×185 mm long ×90 mm thick) grouted masonry prisms were constructed and grouted during each construction stage (a total of 30 prisms). These prisms were later tested, in accordance with CSA S304.1 (CSA 2004b), to determine the masonry compressive strength as well as the ultimate compressive strain. The average compressive strength of the grouted masonry prisms, f'_m, was 16.4 MPa (*c.o.v. = 16.3%)*. This strength is equivalent to 18.8 MPa for two-block high prisms, specified by ASTM C1314 (2006). Tension tests were conducted on the reinforcement to determine the yield strength for the steel used in wall construction. Five tensile specimens, 600 mm long, of M10, D4, and the 3 mm smooth bars, used for the vertical, the horizontal, and the spiral reinforcement, respectively, were tested to determine the reinforcement characteristics. Stress-strain curves for the tested reinforcement showed no well-defined yield point for the vertical reinforcement used in the walls. An elastic-plastic idealization of the bars was conducted and resulted in average yield strength of the bars of 495 MPa (*c.o.v.* = 2.4%), using an average Young's modulus of 200.6 GPa (*c.o.v.* = 2.2%). The average yield strength of the D4 bars and the smooth spiral reinforcement were 534 MPa and 698 MPa, respectively, based on cross section areas equal to 25.4 mm^2 and 10.1 mm^2, respectively.

TEST PROCEDURE

Testing started by in-plane loading each wall to reach specific load levels specified as fractions of the theoretical yield resistance of that wall, Q_y. After reaching the actual yield displacement, Δ_y, (based on the strain gauge reading of the outermost bar at the wall-foundation interface), loading was based on target multiples of Δ_y, where, at each new displacement level, two full loading cycles were applied. This displacement-controlled loading continued until each wall lost about 50% of its maximum lateral load resistance, Q_u, which was considered the failure criterion in this study.

LATERAL LOAD CAPACITY

The response of all walls is discussed based on the lateral load resistance for both the (+)ve and (-)ve cycles corresponding to initial yield of tension reinforcement, Q_y, wall ultimate resistance, Q_u, and 20% strength degradation, $Q_{0.8u}$.The predicted and experimentally measured yield strength, Q_y, and ultimate flexural strength, Q_u, of all walls are listed in Table 2. Strength predictions were carried out by including compression reinforcement, even though North American design codes recommend ignoring compression reinforcement unless it is adequately tied. Shedid el al. (2008) demonstrated that including the compression reinforcement in capacity prediction of RM shear walls results in better agreement with the experimental results than when the influence of compression reinforcement is neglected.

Table 2: Summary of Predicted and Measured Wall Strengths

Specimen	Q_y (kN)				Q_u (kN)				V_u (kN)			
	Predicted		Measured		Predicted		Measured		Outside plastic hinge zone		Inside plastic hinge zone	
	S304.1 (2004)	MSJC (2011)	(+) ve	(-) ve	S304.1 (2004)	MSJC (2011)	(+) ve	(-) ve	S304.1 (2004)	MSJC (2011)	S304.1 (2004)	MSJC (2011)
Phase I												
W1	95	98	101	110	170	169	177	180	206	217	136	59
W2	122	123	121	123	163	162	151	154	198	210	135	59
W3	123	124	110	106	165	164	152	147	198	210	135	59
Phase II												
W4	142	147	160	162	254	253	265	267	406	384	340	228
W5	182	183	185	183	244	242	245	239	400	378	337	228
W6	183	184	173	169	246	246	241	234	400	378	337	228
W7	183	184	188	170	246	246	240	236	400	378	337	228

Using beam analysis with strain proportional to distance from the neutral axis, the strength predictions were carried out using CSA S304.1 (2004b) and the MSJC code (2011) without material or strength reduction factors applied. There are three main differences in these analyses. In CSA S304.1, the equivalent rectangular stress block uses a stress of 0.85 f'_m whereas 0.80 f'_m is used in the MSJC code. Both codes use a depth of the rectangular stress block equal to 80% of the distance to the neutral axis. In the CSA S304.1, the limiting extreme fibers compressive strain is 0.003 compared to 0.0025 in the MSJC code. Finally, in the CSA S304.1 predictions, the compressive strength of 16.4 MPa was taken directly from tests of 4-block high prisms. However, since the masonry compressive strength in the MSJC corresponds to prisms with a height to thickness ratio of 2.0 (ASTM C1314, 2006), the 16.4 MPa strength was adjusted to 18.8 using a height adjustment factor of 1.15.

The experimental results in Table 2 are compared to the predicted values using both the Canadian (CSA, 2004b) and American (MSJC, 2011) design codes. Despite the higher masonry compressive strength, used for ultimate strength predictions (18.8 MPa for the MSJC versus 16.4 MPa in the CSA S304.1), and the higher modulus of elasticity, used for resistance at yield calculations (900×18.8 for the MSJC code versus 850×16.4 in the CSA S304.1), both codes closely predict the measured values. In general, the results in Table 2 indicate that the use of beam theory results in accurate flexural strength predictions of flanged and end-confined RM shear walls as well as that of rectangular walls. This indicates that such construction category (flanged and end-confined walls) can be easily adopted in North American codes with almost no modifications to existing strength calculation clauses pertaining to rectangular walls.

Predicted shear strength, V_u, presented in Table 2, is also calculated following the CSA S304.1 (2004) and the MSJC code (2011) without strength or material reduction factors. The maximum shear strength limit specified by both codes to avoid diagonal compression failure was ignored during the design phase. By assuming that the total length and the thickness of the web resist the entire shear force, the nominal shear strength calculated following the MSJC code (2011) for the test walls is 210 kN and the maximum shear strength calculated following the CSA S304.1 is 236 kN. Test results of W4, reaching a strength of about 270 kN without shear failure, indicate that the limiting shear strength values in North American codes may be somewhat conservative (Miller el al., 2005). Predicted shear strength values for the test walls within the plastic hinge region were calculated to avoid any premature shear failure in these zones and are also presented in Table 2. It is worth noting that the American code neglect the contribution of the masonry in the plastic hinge zone whereas, the Canadian code accounts for 50% reduction in masonry shear strength.

DISPLACEMENT CAPACITIES

Table 3 contains the measured lateral displacements for all walls at the onset of yield of the outermost bar, Δ_y, at maximum load, Δ_u, and at 20% strength degradation in the post-peak stage, $\Delta_{0.80u}$. The table also gives the wall secant stiffness values (as a percentage of the initial transformed stiffness) at each displacement level to show the evolution of the lateral wall stiffness degradation with increased top wall displacement.

Table 3: Measured Displacements and Calculated Stiffness and Ductility Values

Specimen	Direction	Measured displacements and corresponding stiffness						Displacement ductility, [μ_Δ]						
		At first yield		At Maximum load		At 20% strength degradation		At Maximum load		At 1% drift		At 20% strength degradation		
		Δ_y* (mm)	K_y ($\%K_G$)	Δ_u (mm)	K_u ($\%K_G$)	$\Delta_{0.80u}$ (mm)	$K_{0.8u}$ ($\%K_G$)	$\mu_{\Delta u}$	% drift	$\mu_{\Delta 1\%}$	$\mu^{ep}_{\Delta 1\%}$	$\mu_{\Delta 0.8u}$	% drift	$\mu^{ep}_{\Delta 0.8u}$
Phase I														
W1	(+) ve	8.5	44	25.1	25	45.0	11	3.0	0.63	4.7	2.7	5.3	1.13	3.0
	(-) ve			25.3	25	48.0	11	3.0	0.63		2.9	5.6	1.20	3.5
W2	(+) ve	10.5	30	31.5	12	70.0	5	3.0	0.79	3.8	3.0	6.7	1.75	5.3
	(-) ve			31.5	13	68.0	5	3.0	0.79		3.0	6.5	1.70	5.2
W3	(+) ve	9.2	31	36.0	11	93.0	3	3.9	0.90	4.3	3.1	10.1	2.33	7.3
	(-) ve			36.1	11	95.0	2	3.9	0.90		3.1	10.3	2.38	7.4
Phase II														
W4	(+) ve	3.5	58	14.1	24	27.0	10	4.0	0.53	7.6	4.6	7.7	1.02	4.6
	(-) ve			12.5	26	28.0	10	3.6	0.47		4.7	8.0	1.05	4.9
W5	(+) ve	5.0	36	14.6	16	42.0	4	2.9	0.55	5.3	4.0	8.4	1.58	6.3
	(-) ve			25.1	9	45.0	4	5.0	0.94		4.1	9.0	1.69	6.9
W6	(+) ve	4.0	42	24.1	10	52.0	4	6.0	0.91	6.7	4.8	13.0	1.95	9.3
	(-) ve			24.0	10	57.0	3	6.0	0.90		4.8	14.3	2.14	10.3
W7	(+) ve	5.0	35	20.1	12	62.0	3	4.0	0.76	5.3	4.2	12.4	2.33	9.7
	(-) ve			20.0	12	67.0	3	4.0	0.75		3.8	13.4	2.52	9.7

* **Values based on the first onset of yielding recorded in the outermost bar at wall-foundation interface (average for both directions)**

For walls tested in each phase, the measured displacements at first yield, Δ_y, did not vary significantly compared to displacement variations at maximum load, Δ_u, and at 20% strength degradation, $\Delta_{0.8u}$, as presented in Fig. 2 (a) and (b), respectively. The yield displacements ranged between 0.21% and 0.26% drift for the 3-storey walls and between 0.13% and 0.19% drift for the 2-storey walls. Displacements at ultimate load ranged, on average, between 0.47% and 0.91% drift for the test walls with the lowest and highest values corresponding to the rectangular wall specimen W4 and the end-confined wall specimen W6, respectively. For both wall aspect ratios tested (1.5 and 2.2), the drift ratios at 20% strength degradation were at least 1.0%, 1.5%, and 2.0% corresponding to the rectangular, the flanged, and the end-confined walls, respectively. The results show that the proposed modifications to the rectangular wall ends did not significantly affect the wall displacements at first yield; however it significantly increased the attained displacements (drift level) prior to any significant loss in lateral wall capacity. The NBCC (2010) also specifies 1% drift as the displacement limit for *Post-disaster buildings*, which are required to be fully-operational after seismic events, with little or insignificant strength degradation and 2.5% drift for buildings if normal importance. On the other hand, the ASCE-7 (2010) specifies a maximum drift level of 1% drift for masonry cantilever shear walls structures and up to 2.5% drift for other structures.

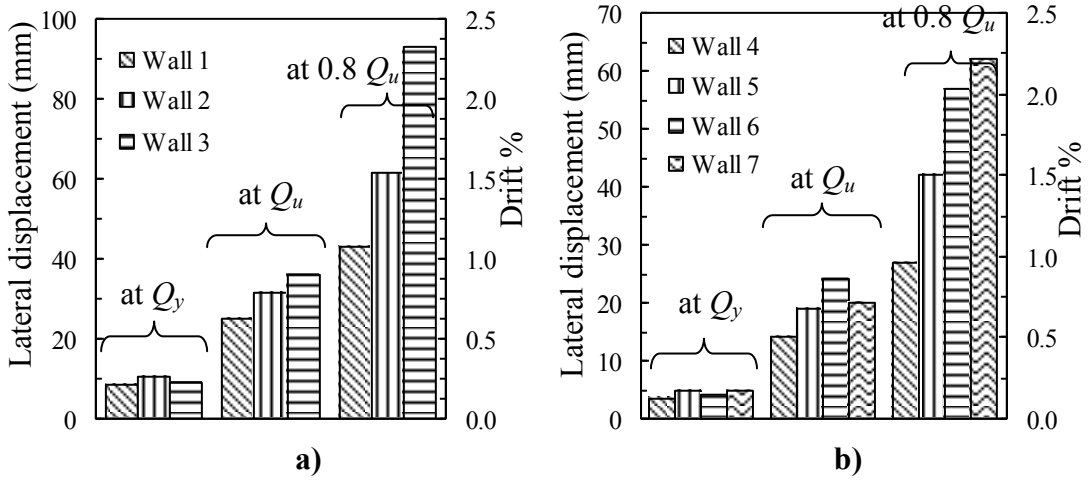

Fig. 2: Effect of end configuration on wall displacements, a) Walls in Phase I, b) Walls in Phase II

The envelopes of the load-displacement relationships for the test specimens in Phases I and II are presented in Fig. 3. The displacement capabilities of rectangular walls are significantly enhanced as a result of the proposed modification to the wall end zone. The drift level attained by the flanged and the end-confined walls at 20% strength degradation were, respectively, 50% and 100% higher to those of the rectangular walls.

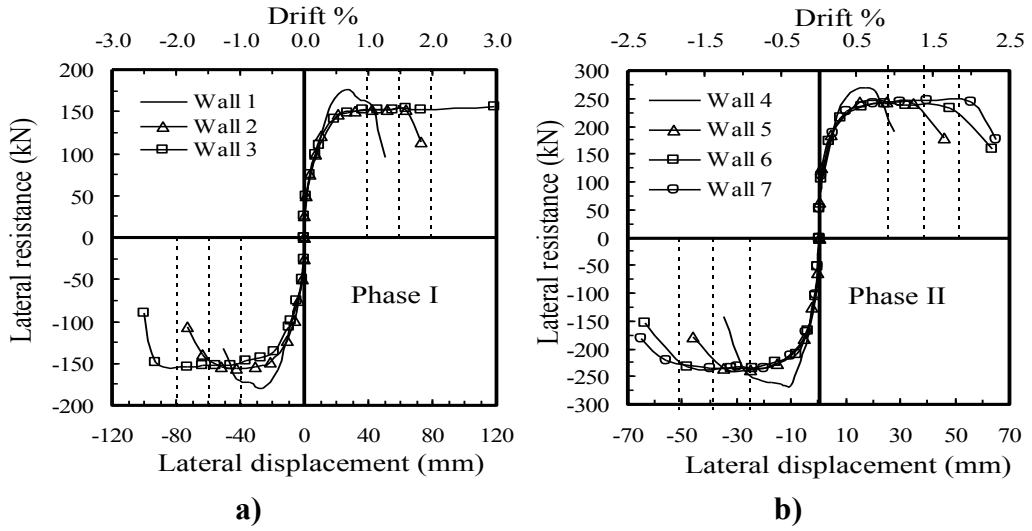

Fig. 3: Load-displacement Relationships, a) Walls in Phase I, b) Walls in Phase II

It can also be seen from the figures that the stiffness of all specimens tested in the same phase remained very similar until the onset of yielding. Having all the walls with almost same stiffness implies that the design seismic force, assuming elastic behavior, should be the same for all walls. However, as the seismic demand is affected by the ductility capacity, the seismic design force should be significantly reduced for the flanged and end-confined walls compared to rectangular walls. In addition, the level of lateral inelastic strength demand is influenced by the ductility capacity (Miranda and Bertero, 1994) and, as a consequence, the design lateral force could be reduced for the flanged and end-confined walls compared to rectangular walls. In addition to the significant enhancement in ductility and drift capacities, a saving of more than 40% in the amount of vertical reinforcement resulted from adopting the proposed strategies.

DUCTILITY CHARACTERISTICS

The measured displacement ductility, μ_{Δ}, is defined herein as the ratio between the measured top displacement at a specified limit and the experimentally-measured displacement at the onset of yield of the outermost vertical bar without any idealization to the load-displacement relationship. The measured displacement ductilities, $\mu_{\Delta u}$, $\mu_{\Delta 1\%}$, and $\mu_{\Delta 0.8u}$ at ultimate load, 1% drift, and 20% strength degradation, respectively, are listed in Table 3.

Measured displacement ductility values at ultimate load, $\mu_{\Delta u}$, ranged between 3.0 and 3.9 and between 5.3 and 10.3 at 20% strength degradation, $\mu_{\Delta 0.8u}$, for the 3-storey rectangular (W1) and end-confined (W3) walls, respectively. On the other hand, for the 2-storey rectangular (W4) and end-confined (W6) walls, the measured displacement ductility values ranged between 3.6 and 6.0 at ultimate load and between 7.7 and 14.3 at 20% strength degradation, respectively. A significant enhancement in the ductility capabilities at 20% strength degradation of the proposed end-confined walls compared to the rectangular ones is obvious from the test results. The ductility of the proposed end-confined walls is almost twice that of the corresponding rectangular wall having almost the same lateral capacity and about 60% the amount of vertical reinforcement (11 versus 19 bars).

The idealized yield displacement is herein assumed equal to the product of the measured yield displacement and the ratio of the maximum capacity to the yield strength of the wall (presented earlier in Table 2). The idealized displacement ductility values, $\mu^{ep}_{\Delta 1\%}$ and $\mu^{ep}_{\Delta 0.8u}$, for displacement limits corresponding to 1% drift and 20% strength degradation respectively, are presented in Table 3 and are also shown in Fig. 4. On average, an increase of 62% and 130% in the $\mu^{ep}_{\Delta 0.8u}$ value was achieved by the 3-storey flanged and end-confined walls, respectively, compared to the rectangular Wall W1. The $\mu^{ep}_{\Delta 0.8u}$ values of the 2-storey flanged and end-confined walls were 39% and 16% higher than those of the rectangular Wall W4.

Following a simple equal displacement approach to determine seismic force reduction factors as used in the NBCC (2010), the ductility related force modification factor, R_d, used in seismic design to account for ductility and energy dissipation, can for simplicity be equal to the calculated values $\mu^{ep}_{\Delta 0.8u}$. It can be seen that the calculated R_d values for the rectangular walls are at least 2.9 which exceeds the maximum R_d values (= 2.0) specified by the code for the most ductile shear wall category. This indicates that the rectangular RM walls can provide higher ductility capabilities than those assumed by the Canadian code. Moreover, the proposed wall categories, if included in the code, shall be assigned higher R_d values.

The test results clearly show that rectangular reinforced concrete block shear walls can indeed develop high ductility capabilities and reach high lateral displacement with minor strength degradation. Moreover, a significant gain in ductility capabilities and saving in vertical reinforcement can be achieved using the proposed modifications to the wall end regions.

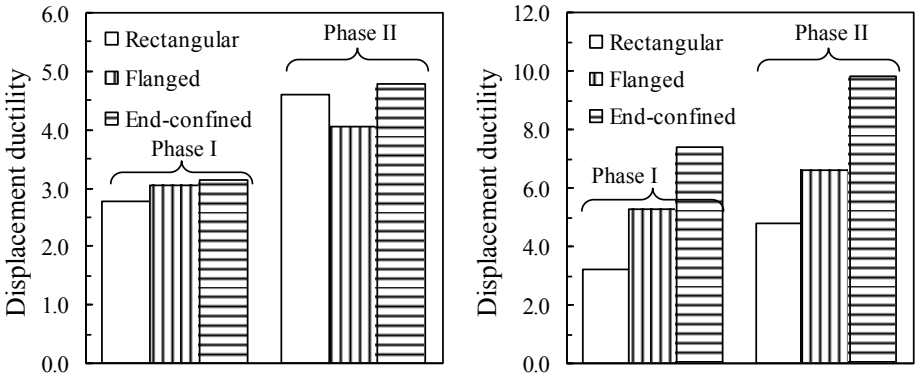

Fig. 4: Displacement ductility capacities for the test specimens at, a) 1% drift; and b) 20% strength degradation

CONCLUSIONS

The performance of reinforced masonry shear walls with different end configurations and aspect ratios is investigated. Seven reinforced concrete-block shear walls were tested under displacement-controlled quasi-static cyclic loading. The test specimens were rectangular, flanged, and end-confined walls having aspect ratios of 2.2 and 1.5. Strength predictions for the walls using both the American and Canadian codes were in excellent agreement with the experimental results when the compression reinforcement was accounted for. This means that the proposed alternative construction strategy can be easily adopted in current codes with minimal modifications to existing strength calculation clauses pertaining to rectangular walls.

The test results showed that all the walls tested within each phase had almost the same capacity, and the same elastic stiffness when subjected to the same axial loads. However, not only a saving of more than 40% in amount of vertical reinforcement was achieved, but a significant enhancement in ultimate displacements and ductility was attained by the flanged and end-confined walls. This shows that, while the elastic seismic forces for the flanged and end-confined walls would remain the same for all walls, a higher seismic reduction factor should be used for these walls compared to that of rectangular walls as a result of the increased ductility. For both aspect ratios tested (2.2 and 1.5), drifts at 20% strength degradation were at least 1.0%, 1.5%, and 2.0% corresponding to the rectangular, flanged, and end-confined walls, respectively. The ductilities of the proposed flanged and end-confined masonry walls were at least 39% and 106% higher than that of the rectangular walls having the same properties for both aspect ratios tested in this study. This indicates that the use of flanged and end-confined walls would be very beneficial in high seismic zones.

The substantially improved performance of the flanged and confined walls was achieved through the use of only one more block at each end of the wall without changing the overall wall length (i.e. by creating flanges or boundary elements). In fact, oftentimes cross walls already exist in the floor layout and flanges can be created simply by proper detailing. Moreover, this cost of the extra blocks would be more than offset by the elimination of 8 of the 19 bars used in the rectangular wall. In addition, the reduced seismic design forces on flanged walls and walls with boundary elements (and the associated material and labor saving) would significantly increase the competitiveness of the proposed alternative construction strategies. The proposed end geometries can be implemented in RM construction with minimal impact on the architectural or the construction practices and can be used mainly in the lower floors (where seismically-induced moments are high). Unlike the common perception that RM shear walls are not ductile, the reported test results demonstrate the high ductility and energy dissipation capacities of reinforced masonry which was accompanied by little strength degradation up to significant drift levels.

ACKNOWLEDGEMENTS

Financial support has been provided by the McMaster University Centre for Effective Design of Structures (CEDS) funded through the Ontario Research and Development Challenge Fund (ORDCF) as well as the Natural Sciences and Engineering Research Council (NSERC) of Canada. Provision of mason time by Ontario Masonry Contractors Association (OMCA) and Canada Masonry Design Centre is appreciated. The supply of half-scale blocks by the Canadian Concrete Masonry Producers Association (CCMPA) is gratefully acknowledged.

REFERENCES

American Society of Civil Engineers (ASCE 2010), *"Minimum design loads for buildings and other structures."* ASCE-7, American Society of Civil Engineers, Reston, Virginia, USA.

American Society for Testing and Material (ASTM). *"Standard test method for compressive strength of masonry prisms."* C1314-06, West Conshohocken, PA.

Canadian Standards Association (CSA 2004a). "*CSA A165: CSA Standards on concrete masonry units,"* CSA, Mississauga, ON, Canada.

Canadian Standards Association (CSA 2004b). "*CSA S304.1-04: Design of masonry structures"*. CSA, Mississauga, ON, Canada.

Eikanas, I. (2003), *"Behaviour of concrete masonry shear walls with varying aspect ratio and flexural reinforcement."* M.A.Sc. Thesis, Department of Civil and Environmental Engineering, Washington State University, USA.

Masonry Standards Joint Committee (MSJC 2011). "Building code requirements for Masonry Structures," TMS 402/ASCE 5/ACI 530, The Masonry Society, American Society of Civil Engineers, & American Concrete Institute, Boulder, New York, & Detroit.

Miller, S., El Dakhakhni, W., and Drysdale, R. (2005). *"Experimental evaluation of the shear capacity of reinforced masonry shear walls."* 10th Canadian Masonry Symposium, University of Calgary, Banff, Alberta, Canada, June 8 – 12

Miranda, E., Bertero, V. (1994). "*Evaluation of strength-reduction factors for earthquake-resistant design"*. Earthquake Spectra, 10(2), 357-379.

NBCC (2010), National Building Code of Canada, Institute for Research in Construction, National Research Council of Canada, Ottawa, ON.

Park, R. and Paulay, R. (1975). *"Reinforced concrete structures."* John Wiley and Sons, New York, N.Y.

Paulay, T. and Priestley, M. (1992). *"Seismic design of reinforced concrete and masonry buildings."* John Wiley and Sons, New York, N.Y.

Priestley, M. (2000). "*Performance based seismic design."* Proceedings 12th World Conference Earthquake Engineering.

Priestley, M., Seible, F., and Calvi, G. (1996). *"Seismic design and retrofit of bridges."* John Wiley and Sons Inc., New York, N.Y.

Priestley, N., Calvi, G., and Kowalsky, M., (2007). *"Displacement-Based Seismic Design of Structures."* IUSS Press, Pavia, Italy.

Seible, F., Hegemier, G., Priestley, M., Kingsley, G., Igarashi, A., and Kurkchubasche A. (1993), "*Preliminary results from the TCCMAR 5- storey full scale reinforced masonry research building test*." Masonry Society Journal, Vol. 12, No.1.

Shedid, M., Drysdale, R., and El-Dakhakhni, W., (2008) "*Behavior of Fully Grouted Reinforced Concrete Masonry Shear Walls Failing in Flexure: Experimental Results"* J. Struct. Engrg. (134)11, 1754-1767

Shedid, M.T., El-Dakhakhni, W. W.and Drysdale, R.G. (2010) "*Seismic Response Parameters of Reinforced Concrete-Block Shear Wall Construction*", ASCE Journal of Performance of Constructed FacilitiesVol. 24, No. 1, pp. 4-18.

Shing, P., Noland, J., Klamerus, E., and Spaeh., H. (1989). "*Inelastic behavior of concrete masonry shear walls*." J. Struct. Eng., (115)9, 2204-2225.

Shing, P., Schuller, M., and Hoskere, V. (1990). "*In-plane resistance of reinforced masonry shear walls*." J. Struct. Eng., (116)3, 619-640.

Tomazevic, M. (1998). *"Earthquake-Resistant Design of Masonry Buildings"* Imperial College Press, Covent Garden, London, UK.